

# Supplemental Material: Point-Based Neural Rendering with Per-View Optimization

## 1. Derivation of probability-based depth

Following from the discussion in Sec. 3.3 in the main paper, we assume  $D_n$  follows distribution  $\mathcal{DF}$  based on a mixture model with density  $\mathcal{DF}_{D_n}(d)$ . We first assume that there exists at least one such point (thus the symbol  $\exists$ ):

$$\mathcal{DF}_{D_n}^\exists(d) = \sum_{i \in \mathcal{N}_n} f(d, d_{n,i}) \left( \alpha_{n,i} \prod_{j=1}^{i-1} (1 - \alpha_{n,j}) \right)$$

$$\mathcal{DF}_{D_n}^\exists(d) = \sum_{i \in \mathcal{N}_n} f(d, d_{n,i}) \beta_{n,i} \quad (1)$$

With:

$$\beta_{n,i} = \alpha_{n,i} \prod_{j=1}^{i-1} (1 - \alpha_{n,j})$$

where  $f(d, d_{n,i}, \sigma_{n,i})$  is the pdf of a distribution that describes the likelihood of point  $p_{n,i}$  being at depth  $d$ . This can be an arbitrary single mode distribution such as a uniform or normal distribution. The distribution of Eq. 1 does not integrate to one, because there is also a probability that no points exist at that pixel for that view:

$$p_{D_n}^\emptyset = \prod_{i \in \mathcal{N}_n} (1 - \alpha_{n,i}) = \beta_{n,\infty}$$

We thus complete  $\mathcal{DF}_{D_n}^\exists(d)$  with a point at infinity to make it a probability density function. In order to simplify the remaining derivations we keep the notation  $\mathcal{N}_n$  for the set of splats from input view  $n$  completed with that point at infinity, and use the corresponding  $\beta_{n,\infty}$  for this point, leading to:

$$\mathcal{DF}_{D_n}(d) = \sum_{i \in \mathcal{N}_n} f_i(d, d_{n,i}) \beta_{n,i}$$

Note that implementation-wise adding the point at infinity is important to avoid corner cases. We can then compute the probability that the (projected) depth of a view  $n$  is smaller than all of the other views:

$$P(D_n < \min_{m \neq n}(D_m)) = \int_{-\infty}^{+\infty} P(t < \min_{m \neq n}(D_m) | D_n = t) \mathcal{DF}_{D_n}(t) dt$$

We have:

$$P(D_n < \min_{m \neq n}(D_m)) = \int_{-\infty}^{+\infty} P(t < \min_{m \neq n}(D_m) | D_n = t) \mathcal{DF}_{D_n}(t) dt$$

$$P(D_n < \min_{m \neq n}(D_m)) = \int_{-\infty}^{+\infty} \prod_{m \neq n} P(t < D_m) \mathcal{DF}_{D_n}(t) dt$$

$$P(D_n < \min_{m \neq n}(D_m)) = \sum_{i \in \mathcal{N}_n} \beta_{n,i} \int_{-\infty}^{+\infty} \prod_{m \neq n} P(t < D_m) f_i(t, d_{n,i}) dt$$

$$P(D_n < \min_{m \neq n}(D_m)) = \sum_{i \in \mathcal{N}_n} \beta_{n,i} \int_{-\infty}^{+\infty} \prod_{m \neq n} \left( \int_t^{\infty} \sum_{j \in \mathcal{N}_m} f_j(s, d_{m,j}) \beta_{m,j} ds \right) f_i(t, d_{n,i}) dt$$

$$P(D_n < \min_{m \neq n}(D_m)) = \sum_{i \in \mathcal{N}_n} \beta_{n,i} \int_{-\infty}^{+\infty} \prod_{m \neq n} \left( \sum_{j \in \mathcal{N}_m} \beta_{m,j} \int_t^{\infty} f_j(s, d_{m,j}) ds \right) f_i(t, d_{n,i}) dt$$

Thus:

$$P(D_n < \min_{m \neq n}(D_m)) = \sum_{i \in \mathcal{N}_n} \beta_{n,i} \int_{-\infty}^{+\infty} \prod_{m \neq n} \left( \sum_{j \in \mathcal{N}_m} \beta_{m,j} \int_t^{\infty} f_j(s, d_{m,j}) ds \right) f_i(t, d_{n,i}) dt$$

A natural candidate for  $f$  would be a normal distribution. Unfortunately this expression would be very costly to compute and does not have a closed form solution. Instead we use a simple symmetric triangle distribution of support  $2\sigma$ , which is easy to evaluate. Example plots of these distributions are presented in Fig. 1. This gives  $f_i$ :

$$f_i(s, d_{n,i}) ds = \begin{cases} \frac{\sigma - |t - x|}{\sigma^2} & \text{if } d_{n,i} - \sigma < t \leq d_{n,i} + \sigma, \\ 0 & \text{otherwise} \end{cases}$$

And:

$$\int_t^\infty f_i(s, d_{n,i}) ds = T(t, d_{n,i}, \sigma) = \begin{cases} 1 & \text{if } t < d_{n,i} - \sigma, \\ 0 & \text{if } t > d_{n,i} + \sigma, \\ 1 - \frac{(x-t+\sigma)^2}{2\sigma^2} & \text{if } d_{n,i} - \sigma < t \leq d_{n,i}, \\ \frac{(t+\sigma-x)^2}{2\sigma^2} & \text{if } d_{n,i} < t \leq d_{n,i} + \sigma, \end{cases}$$

$$P(D_n < \min_{m \neq n}(D_m)) =$$

$$\sum_{i \in \mathcal{N}_n} \beta_{n,i} \int_{d_{n,i}-\sigma}^{d_{n,i}+\sigma} \prod_{m \neq n} \left( \sum_{j \in \mathcal{N}_m} \beta_{m,j} T(t, d_{m,j}, \sigma) \right) f_i(t, d_{n,i}) dt$$

This functional still has no simple closed form formula, so we approximate it with numerical integration:

$$P(D_n < \min_{m \neq n}(D_m)) \approx$$

$$\frac{2\sigma}{S} \sum_{i \in \mathcal{N}_n} \beta_{n,i} \sum_{t=1}^S \prod_{m \neq n} \left( \sum_{j \in \mathcal{N}_m} \beta_{m,j} T(s(t), d_{m,j}, \sigma) \right) f_i(s(t), d_{n,i}) \quad (2)$$

With:

$$s(t) = d_{ni} - \sigma + \frac{t}{S+1}, \text{ and } S \text{ the number of samples}$$

In our experiments, we found that setting  $S = 1$  provided satisfactory results in all our tests. This computation is done in parallel per pixel using CUDA.

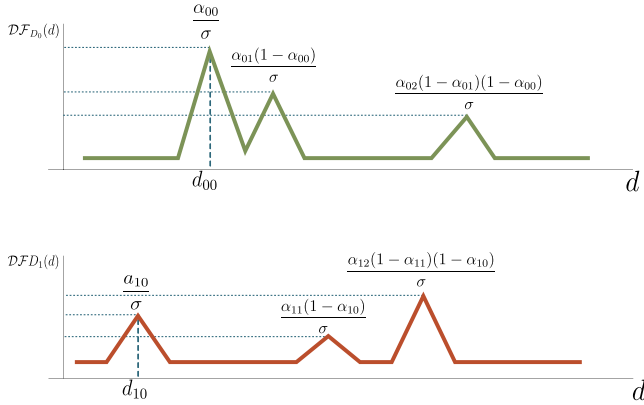


**Figure 1:** Simplified example of two pdfs of a pixel for view  $I_0$  and  $I_1$ . Our soft depth test is the computation of the probability of the random variable  $D_i$  drawn by its corresponding PDF,  $\mathcal{DF}_{D_i}$  shown above, to have a smaller depth than all other  $D_j$ .

## 2. Multi-view Harmonization details

In Fig. 2, we illustrate the evolution of the optimization of  $\mu_i$ .

## 3. Additional Results and Comparisons

In Fig. 3 we show comparisons of our method with two baseline methods, ULR and Textured Mesh.

In Fig. 4 we see that lowering the size of the model often does

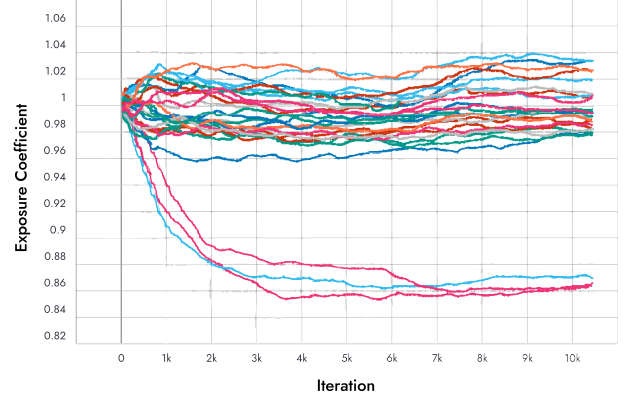


**Figure 2:** The optimization of the  $\mu_i$  for each view for 10k iterations during training of "Ponche" scene. Each line with a different color corresponds to a different input view; we clearly see a group of three images that are brighter (see Fig. 7 in the main paper).



**Figure 3:** Left to right: Unstructured Lumigraph Rendering, Textured Mesh, and our method.

not affect the results substantially and higher number of cameras used for rendering in the same time/memory budget compensates for the smaller neural renderer.

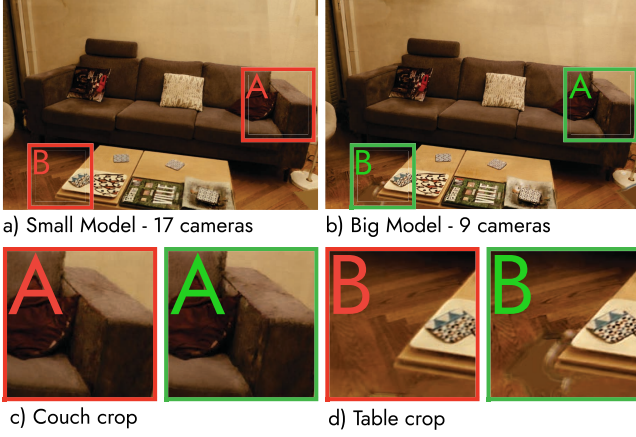


**Figure 4:** In this challenging indoor scene, we use the small neural network to use a larger number of cameras.

**Table 1:** *Quantitative analysis for the full rendering pipeline against the interactive approximation in the paper. For this experiment both methods use a smaller model to allow the latter for interactive frame-rates and isolate the impact of the point splatting approximation.*

	MSE ↓
Museum	0.007
Ponche	0.004
Stairs	0.006
Street	0.008